# Minimum Redundancy Planar Coarrays for High-Resolution MIMO Radar Imaging

*Moein Ahmadi*[†]*, Björn Ottersten*[†]*, Bhavani Shankar M. R.*[†]*, Thomas Stifter*[‡]

[†]Interdisciplinary Centre for Security, Reliability and Trust (SnT), University of Luxembourg, [‡]IEE S.A.

## ABSTRACT

This paper presents a minimum redundancy planar coarray design for high-resolution MIMO radar imaging. By leveraging sparse antenna configurations, the proposed approach enhances angular resolution while minimizing redundant spacings in the virtual array. A joint range-Doppler estimator is developed based on a four-dimensional transmit-receive signal model, facilitating multi-target localization in azimuth and elevation. To minimize the spatial sampling requirements, a combinatorial formulation is introduced for designing planar MIMO minimum redundancy arrays, ensuring a continuous coarray structure with fewer physical elements and exploiting filled coarray locations with FFT-based angle spectra for markedly enhanced computational efficiency over adaptive techniques and sparse recovery methods. Numerical simulations demonstrate that the proposed coarray-based MIMO radar achieves superior resolution compared to conventional filled arrays while effectively suppressing grating lobes. This work provides a cost-efficient solution for high-precision radar imaging applications.

***Index Terms—*** Angle Estimation, Distributed Aperture Radar, High-Resolution Imaging, Sparse Array Design, MIMO Radar, Minimum Redundancy Coarray, Virtual array.

## 1. INTRODUCTION

Multiple-Input Multiple-Output (MIMO) radar has emerged as a critical technology for high-resolution imaging and target detection applications due to its large virtual array and its ability to exploit waveform diversity and spatial processing gains [1–3]. Traditional Uniform Linear Array (ULA), Uniform Rectangular Array (URA) and Uniform Planar Array (UPA) designed for virtual arrays have been extensively utilized in MIMO radar systems; however, the angular resolution is limited by the virtual array aperture and suffers from redundancy in spatial sampling [4]. To address these challenges, sparse linear coarrays have been investigated as an efficient alternative, leveraging non-uniform element distributions to achieve higher resolution with fewer physical antennas [5–7].

Sparse array architectures such as co-prime arrays, nested arrays, and Minimum Redundancy Array (MRA) offer increased degrees of freedom by synthesizing a larger aperture through coarray processing [6, 8]. The difference coarray structure generated by these sparse arrays enables superior Direction-of-Arrival (DoA) estimation and enhances target detection capabilities by effectively suppressing grating lobes while maintaining a continuous spatial sampling structure. Recent advancements in distributed aperture radars [9–11] have demonstrated the potential of these architectures in MIMO radar imaging, achieving better spatial resolution with reduced redundancy [4, 11].

To address these challenges, this paper proposes a minimum redundancy planar coarray design for high-resolution MIMO radar imaging. The proposed approach leverages planar sparse array configurations to construct a four-dimensional transmit-receive matrix, enabling high-precision multi-target localization in both azimuth and elevation. By formulating the coarray design as a combinatorial optimization problem, we develop a continuous coarray structure that minimizes redundant spacings while maintaining the necessary spatial sampling diversity. Moreover, the utilization of filled coarray locations combined with Fast Fourier Transform (FFT)-based angle spectrum estimation renders the processing considerably more computationally efficient than adaptive techniques or sparse recovery methods in compressed sensing-based approaches. This results in improved resolution over conventional filled arrays while effectively suppressing grating lobes.

## 2. SIGNAL MODEL

We consider a multichannel Frequency Modulated Continuous Wave (FMCW) radar equipped with a sparse planar array coarray configuration. The system consists of $M$ transmit elements and $N$ receive elements, located at

$$\mathbf{p}_{T,m} = (0, \bar{m}_{y,m}, \bar{m}_{z,m})\,\frac{\lambda}{2}, \quad m = 1, \ldots, M, \tag{1}$$

$$\mathbf{p}_{R,n} = (0, \bar{n}_{y,n}, \bar{n}_{z,n})\,\frac{\lambda}{2}, \quad n = 1, \ldots, N. \tag{2}$$

Here, $(\bar{m}_{y,m}, \bar{m}_{z,m}) \in \mathbb{M}$ and $(\bar{n}_{y,n}, \bar{n}_{z,n}) \in \mathbb{N}$, where $\mathbb{M}$ and $\mathbb{N}$ are sets of integer pairs with cardinalities $|\mathbb{M}| = M$ and $|\mathbb{N}| = N$, respectively.

The received radar data from the environment is captured by each receive antenna, sampled in $K$ fast-time samples and

This work was funded in part, by the Luxembourg National Research Fund (FNR), grant reference INTER/MOBILITY/2023/IS/18014377/MCR.

$LM$ pulses, forming a three-dimensional tensor, referred to as the radar data cube, $\mathbf{T} \in \mathbb{C}^{K\times LM\times N}$. Applying range windowing followed by a fast-time FFT (for FMCW radars) or a matched filter (for pulsed radars) leads to the range-slow time-antenna tensor, $\mathbf{Y} \in \mathbb{C}^{K\times LM\times N}$. A joint Doppler processing and MIMO demodulation approach [12] is then applied to obtain a four-dimensional range-Doppler-transmit-receive tensor, $\mathbf{Z} \in \mathbb{C}^{K\times L\times M\times N}$. After applying range-Doppler Constant False Alarm Rate (CFAR) detection on the following range-Doppler map

$$\mathbf{T} = \sum_{m=1}^{M}\sum_{n=1}^{N} |\mathbf{Z}[:,:,m,n]|^2 \tag{3}$$

Each detection point in $\{(R_k, f_{d,k})\}$, corresponds to a transmit-receive antenna matrix, $\mathbf{Z}_k \in \mathbb{C}^{M\times N}$. It can contain multiple targets at different azimuth and elevation angles.

The phase difference for the $k$-th target at the $(m,n)$-th transmitter-receiver pair is given by:

$$\phi_{k,m,n} = -\frac{2\pi}{\lambda}\left(\|\mathbf{p}_k^t - \mathbf{p}_m^{tx}\| + \|\mathbf{p}_k^t - \mathbf{p}_n^{rx}\|\right), \tag{4}$$

where the target position is parameterized as $\mathbf{p}_k^t = R_k\hat{\mathbf{r}}_k$. Here, $\hat{\mathbf{r}}_k = [\cos\theta_k\cos\phi_k, \sin\theta_k\cos\phi_k, \sin\phi_k]^T$ is the unit direction vector, with $\theta_k$ and $\phi_k$ denoting the azimuth and elevation angles of the target. Using the far-field approximation,

$$\|\mathbf{p}_k^t - \mathbf{p}_m^{tx}\| \approx R_k - \mathbf{p}_m^{tx}\cdot\hat{\mathbf{r}}_k, \tag{5}$$

The phase term can be rewritten as:

$$\phi_{k,m,n} \approx \frac{2\pi}{\lambda}\left(\mathbf{p}_m^{tx} + \mathbf{p}_n^{rx}\right)\cdot\hat{\mathbf{r}}_k - \frac{4\pi}{\lambda}R_k. \tag{6}$$

Since the last term is the same for all transmit-receive pairs, it can be considered as a constant phase offset and removed. The phase used in angle processing is:

$$\varphi_{k,m,n} = \frac{2\pi}{\lambda}\left(\mathbf{p}_m^{tx} + \mathbf{p}_n^{rx}\right)\cdot\hat{\mathbf{r}}_k. \tag{7}$$

### 2.1. Planar Array

For a traditional filled rectangular MIMO radar, the antenna element positions are selected as: $\bar{m}_{y,m} = mN_y$, $\bar{m}_{z,m} = mN_z$; $m = 0,\ldots,M_y-1$, and $\bar{n}_{y,n} = n$, $\bar{n}_{z,n} = n$; $n = 0,\ldots,N_y-1$, and $M_yM_z = M, N_yN_z = N$. For this uniform rectangular MIMO radar, the received signal for a target is:

$$s_{k_y,k_z} = \exp(j\pi(\sin\theta_k\cos\phi_k k_y + \sin\phi_k k_z)), \tag{8}$$

where $k_y$ and $k_z$ denote the indices of the virtual array, and $k_y \in \{\bar{m}_{y,m} + \bar{n}_{y,n}\}$, $k_z \in \{\bar{m}_{z,m} + \bar{n}_{z,n}\}$.

### 2.2. Coarray of URA Virtual Array

The corresponding coarray signal set can be expressed as

$$\{s_{k_y,k_z}s^*_{k'_y,k'_z}\} = \{e^{j\omega_y(k_y-k'_y)}e^{j\omega_z(k_z-k'_z)}\}. \tag{9}$$

Each signal is associated with a coarray antenna location, and these locations may repeat. Specifically, the coarray antenna locations are given by $\mathbb{C}_{\mathbb{M},\mathbb{N}} = \{(\bar{m}_{y,m} + \bar{n}_{y,n} - \bar{m}_{y,m'} - \bar{n}_{y,n'},\ \bar{m}_{z,m} + \bar{n}_{z,n} - \bar{m}_{z,m'} - \bar{n}_{z,n'})\}$.

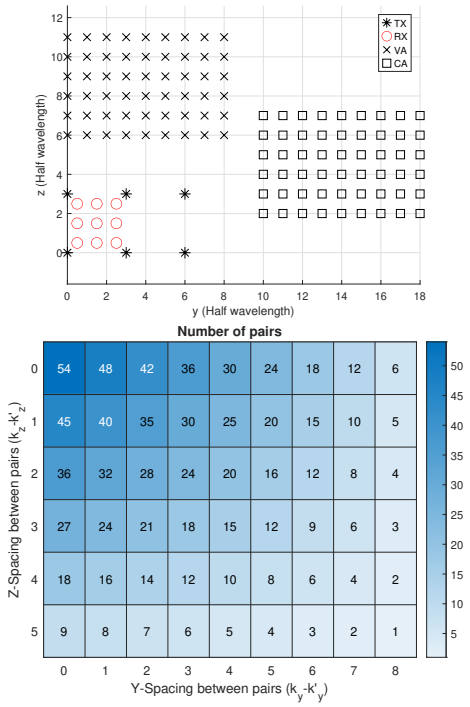


**Fig. 1**: (a) Transmit, receive, virtual, and coarray antenna locations. (b) Histogram of the number of coarray pairs, $\mathbf{C}_{\mathbb{M},\mathbb{N}}$, for a traditional filled URA virtual array MIMO radar ($M = 6, N = 9$).

The two-dimensional pairs histogram, $\mathbf{C}_{\mathbb{M},\mathbb{N}}$, counts how many times each pair appears in the set $\mathbb{C}_{\mathbb{M},\mathbb{N}}$. As illustrated in Fig. 1 for a $U_y \times U_z$ uniform rectangular virtual array (in this example, $9\times 6$), consider a fixed $z$-spacing $D_z$ (with $D_z = 0,\ldots,U_z-1$). In this case, a spacing of one unit along $y$ occurs $(U_z - D_z)(U_y - 1)$ times, a spacing of two units occurs $(U_z - D_z)(U_y - 2)$ times, and the maximum $y$-spacing of $U_y - 1$ occurs only $(U_z - D_z)$ times. By eliminating these redundant spacings, the effective aperture of the array can be increased, while all spatial spacing information is preserved, yielding higher resolution. This idea aligns with the concept of a Minimum Redundancy Array (MRA), which requires that the set of coarray locations, $\mathbb{C}_{\mathbb{M},\mathbb{N}}$, contains a continuous sequence of antenna positions.

### 2.3. Azimuth Angle Resolution

To improve azimuth resolution, without grating lobes, define the subset $\mathbb{L}_{az}(L_y) = \mathbb{L}_{1:L_y,0} = \{(1,0),(2,0),\ldots,(L_y,0)\}$, $\mathbb{L}_{az}(L_y) \subset \mathbb{C}_{\mathbb{M},\mathbb{N}}$ should be satisfied. The corresponding signal array is given by

$$\mathbf{z}_{az}(i) = \frac{1}{\mathbf{C}_{\mathbb{M},\mathbb{N}}(i,0)} \sum_{\substack{\mathbb{C}_{\mathbb{M},\mathbb{N}} \\ k_y - k'_y = i \\ k_z - k'_z = 0}} s_{k_y,k_z}\, s^*_{k'_y,k'_z}, \quad i = 0,1,\ldots,L_y.$$

The nonadaptive azimuth beampattern is then computed by taking the discrete Fourier transform (DFT) of the windowed (e.g., Hamming window) and zero-padded version of $\mathbf{z}_{az}$:

$$\bar{\mathbf{z}}_{az} = \mathbf{F}_{L'_y}\Big[\mathbf{w}_{L_y} \odot \mathbf{z}_{az};\, \mathbf{0}_{L'_y - L_y}\Big], \tag{10}$$

where $\mathbf{F}_{L'_y}$ is the DFT matrix, $\mathbf{w}_{L_y}$ is a window of length $L_y$ (extended to length $L'_y > L_y$ via zero-padding), and $\odot$ denotes element-wise multiplication.

### 2.4. Elevation Angle Resolution

Similarly, to enhance elevation resolution, define

$$\mathbb{L}_{el}(L_z) = \mathbb{L}_{0,1:L_z} = \{(0,1),(0,2),\ldots,(0,L_z)\} \subset \mathbb{C}_{\mathbb{M},\mathbb{N}},$$

with the associated signal array

$$\mathbf{z}_{el}(i) = \frac{1}{\mathbf{C}_{\mathbb{M},\mathbb{N}}(0,i)} \sum_{\substack{\mathbb{C}_{\mathbb{M},\mathbb{N}} \\ k_y - k'_y = 0 \\ k_z - k'_z = i}} s_{k_y,k_z}\, s^*_{k'_y,k'_z}, \quad i = 0,1,\ldots,L_z.$$

The elevation beampattern is obtained similarly as

$$\bar{\mathbf{z}}_{el} = \mathbf{F}_{L'_z}\Big[\mathbf{w}_{L_z} \odot \mathbf{z}_{el};\, \mathbf{0}_{L'_z - L_z}\Big]. \tag{11}$$

### 2.5. Joint Azimuth-Elevation Resolution

For a filled rectangular coarray that enhances both azimuth and elevation resolution, the coarray must include every pair within the rectangular region: $\mathbb{L}_{azel}(L_y,L_z) = \mathbb{L}_{1:L_y,0} \cup \mathbb{L}_{1:L_y,1} \cup \cdots \cup \mathbb{L}_{1:L_y,L_z} \cup \mathbb{L}_{0,1:L_z} \subset \mathbb{C}_{\mathbb{M},\mathbb{N}}$. The associated two-dimensional signal array is defined as

$$\mathbf{Z}(i,j) = \frac{1}{\mathbf{C}_{\mathbb{M},\mathbb{N}}(i,j)} \sum_{\substack{\mathbb{C}_{\mathbb{M},\mathbb{N}} \\ k_y - k'_y = i \\ k_z - k'_z = j}} s_{k_y,k_z}\, s^*_{k'_y,k'_z}.$$

After zero-padding the windowed version $\mathbf{W}_{L_y,L_z} \odot \mathbf{Z}$ to obtain $\mathbf{Z}_{zp}$, the joint azimuth-elevation beampattern is computed as

$$\bar{\mathbf{Z}} = \mathbf{F}_{L'_y}\, \mathbf{Z}_{zp}\, \mathbf{F}^H_{L'_z}.$$

The filled coarray locations and the FFT-based angle spectra make the processing more computationally efficient compared to adaptive techniques [13] or sparse recovery methods in compressed sensing-based approaches [14].

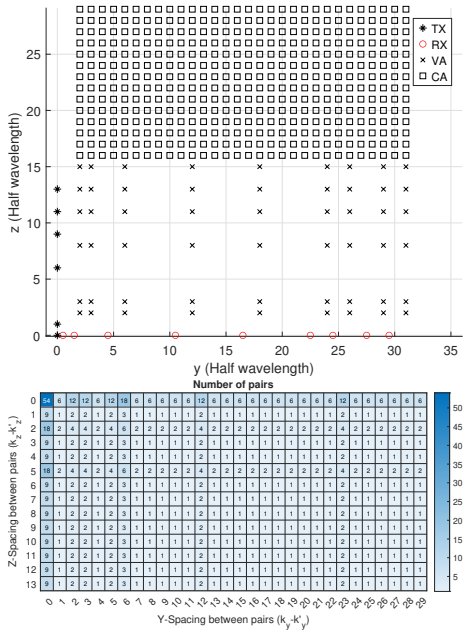


**Fig. 2**: (a) Transmit, receive, virtual, and coarray antenna locations. (b) Histogram of the number of coarray pairs, $\mathbf{C}_{\mathbb{M},\mathbb{N}}$, for the proposed 2D MRA MIMO radar, $\mathbb{L}_{azel}(29,13)$, with $M = 6$ and $N = 9$.

## 3. PLANAR MIMO MINIMUM REDUNDANCY ARRAY DESIGN

To achieve the desired coarray structure, we define the following optimization problem:

$$\begin{aligned} &\underset{\mathbb{M},\mathbb{N}}{\text{minimize}} \quad M + \alpha N, \\ &\text{subject to} \quad \mathbb{L}_{ang}(L_y,L_z) \subset \mathbb{C}_{\mathbb{M},\mathbb{N}}, \\ &\quad |\mathbb{M}| = M, \quad |\mathbb{N}| = N, \end{aligned} \tag{12}$$

where $\alpha$ represents the transmit-receiver cost ratio, which is introduced because the cost of transmit and receive chains may differ due to hardware complexity, power consumption, or implementation constraints, and

$$\mathbb{L}_{ang}(L_y,L_z) \in \Big\{\mathbb{L}_{az}(L_y) \cup \mathbb{L}_{el}(L_z),\, \mathbb{L}_{azel}(L_y,L_z)\Big\}.$$

This problem is combinatorial in nature and, in general, is not easy to solve. For smaller values of $L_y$ and $L_z$, one can employ an exhaustive search algorithm to find the solution. In [5], for one-dimensional SIMO MRA arrays (i.e., $M = 1$, $L_z = 1$, and $\alpha = 1$), a class of linear arrays is presented that achieves maximum resolution for a given number of elements $L_y$ by minimizing the number of redundant spacings present in the array. For example, for $L_y = 23$ the solution is $\mathbb{N} = \{(0,0),(1,0),(4,0),(10,0),(16,0),(18,0),(21,0),(23,0)\}$ with $N = 8$.

In [4], for one-dimensional MIMO MRA arrays ($L_y = 63$, $L_z = 1$, and $\alpha = 1$), a solution is found with $\mathbb{M} =$

$\{(0,0),(1,0),(3,0)\}$ and $\mathbb{N} = \{(0,0),(6,0),(13,0),(40,0),(60,0)\}$ with $M = 3, N = 5$.

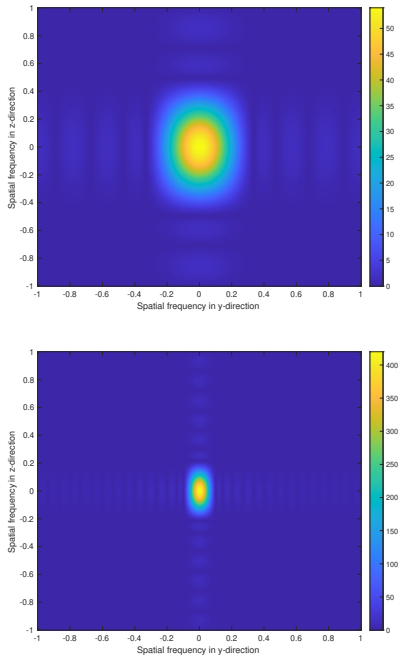


**Fig. 3**: Azimuth-elevation beampattern for $M = 6, N = 9$: (a) Filled virtual array MIMO radar; (b) Filled coarray MIMO radar.

In the planar array case, inspired by these works, the 1D restricted and general coarray designs from [5] are employed to achieve $\mathbb{L}_{azel}(L_y, L_z)$, with transmitters placed along the $y$-direction and receivers along the $z$-direction (or vice versa). Fig. 2 shows the designed array for $\mathbb{L}_{azel}(29, 13)$ which is obtained using the same number of transmit and receive elements as in Fig. 1. Specifically, the array configurations are given by $\mathbb{M} = \{(0,0),(1,0),(4,0),(10,0),(16,0),(22,0),(24,0),(27,0),(29,0)\}$ and $\mathbb{N} = \{(0,0),(0,1),(0,6),(0,9),(0,11),(0,13)\}$.

Fig. 3 shows the azimuth-elevation beampatterns for the conventional filled MIMO array in Fig. 1 and the proposed coarray-based antenna configuration in Fig. 2, where the same number of transmit and receive elements are used. As can be seen, the proposed coarray design has narrower beamwidths without any grating lobes both in azimuth and elevation in comparison with the traditional filled virtual array rectangular MIMO radar.

Inspired by [4], choosing $\mathbb{M} = \{(0,0),(0,1),(1,0),(0,3),(3,0)\}$ and $\mathbb{N} = \{(0,0),(0,6),(6,0),(0,13),(13,0),(0,40),(40,0),(0,60),(60,0)\}$ leads to the achievement of $\mathbb{L}_{1D,63,63}$. Fig. 4 shows the transmit and receive antenna locations, as well as the virtual array and the resulting coarray. Fig. 4(b) presents the coarray pair counts, omitting the pairs with zero counts; as can be seen, only the pair locations along the zero-spacing axes need to be filled.

To evaluate the angle resolution of this coarray configuration, a simulation scenario with three targets is considered. The targets have azimuth and elevation angles of $(0,0)$, $(2,0)$, and $(3,5)$ degrees, respectively. Fig. 5 shows the non-adaptive azimuth and elevation beampatterns as defined in equations 10 and 11. It can be observed that the targets can be resolved in both azimuth and elevation when the proposed planar coarray is used. In contrast, when the same number of transmit and receive antennas are used to form a $9 \times 5$ filled MIMO virtual array, the targets cannot be resolved because they are closer than the azimuth and elevation resolution limits of that array.

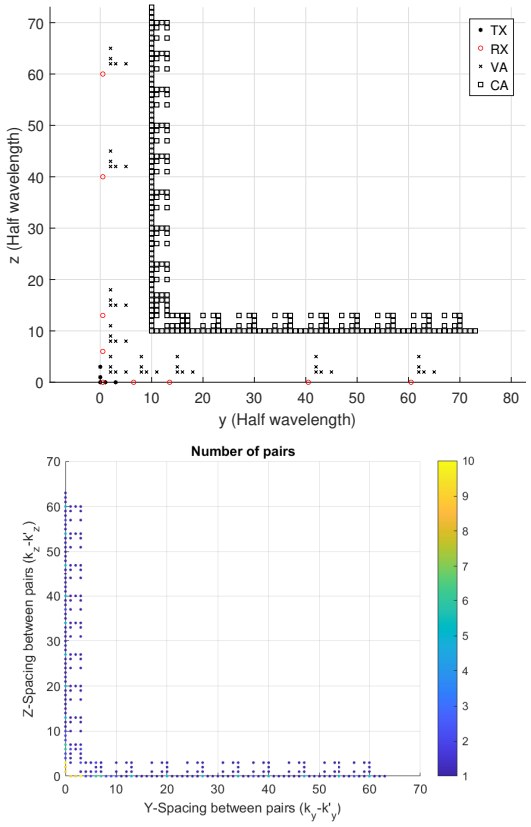


**Fig. 4**: (a) Transmit, receive, virtual, and coarray antenna locations. (b) Histogram of the number of coarray pairs, $\mathbf{C}_{\mathbb{M},\mathbb{N}}$, for the proposed MRA MIMO radar, $\mathbb{L}_{az}(63) \cup \mathbb{L}_{el}(63)$, with $M = 5$ and $N = 9$.

## 4. LIMITATIONS

Although the proposed coarray designs increase angle resolution, the nonlinear nature of the virtual array signal multiplications used to obtain coarray signals introduces several limitations. First, the superposition property is not preserved for multiple targets, which leads to additional parameter estimation errors. Moreover, the noise signal vector is no longer Gaussian, complicating the design of a GLRT detector.

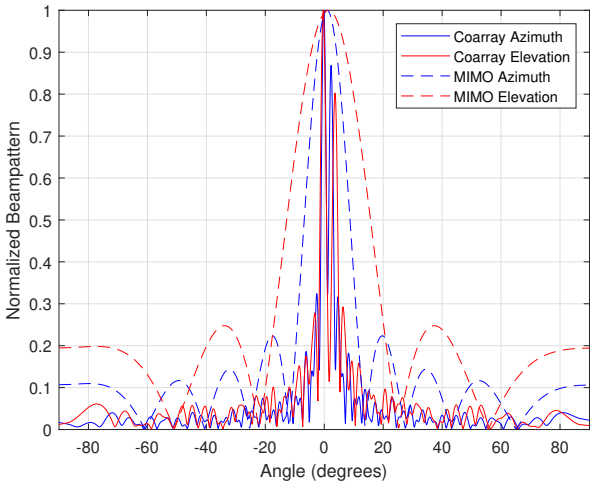


**Fig. 5**: Azimuth and elevation beampatterns for the proposed planar coarray and the traditional filled rectangular MIMO radar, both using $M = 5$ and $N = 9$.

## 5. CONCLUSION

In this paper, we presented a signal processing framework for multichannel FMCW radar systems employing sparse planar coarray configurations. Our approach integrates range-Doppler processing with CFAR detection to construct a transmit-receive matrix, enabling high-resolution multi-target localization in both azimuth and elevation. By leveraging a coarray representation of the received signal, we demonstrated the effectiveness of minimum redundancy arrays (MRA) in enhancing angular resolution for planar MIMO radar architectures. Through the derivation of coarray signal formulations, we illustrated how reducing redundancy in virtual array configurations improves spatial sampling and angular resolution. Additionally, we introduced an optimization framework for designing planar MIMO minimum redundancy arrays, achieving an expanded filled coarray virtual aperture while minimizing the number of physical antennas. Comparative simulations against conventional filled MIMO arrays validated that our proposed coarray-based design attains higher angular resolution, using the same number of elements, while effectively mitigating grating lobes.

## 6. REFERENCES


[1] Shunqiao Sun, Athina P. Petropulu, and H. Vincent Poor, "MIMO radar for advanced driver-assistance systems and autonomous driving: Advantages and challenges," *IEEE Signal Processing Magazine*, vol. 37, no. 4, pp. 98–117, 2020.

[2] Wei Liu, Martin Haardt, Maria S. Greco, Christoph F. Mecklenbräuker, and Peter Willett, "Twenty-five years of sensor array and multichannel signal processing: A review of progress to date and potential research directions," *IEEE Signal Processing Magazine*, vol. 40, no. 4, pp. 80–91, 2023.

[3] Stefano Fortunati, Luca Sanguinetti, Fulvio Gini, Maria Sabrina Greco, and Braham Himed, "Massive mimo radar for target detection," *IEEE Transactions on Signal Processing*, vol. 68, pp. 859–871, 2020.

[4] Chun-Yang Chen and P. P. Vaidyanathan, "Minimum redundancy MIMO radars," in *2008 IEEE International Symposium on Circuits and Systems (ISCAS)*, 2008, pp. 45–48.

[5] A. Moffet, "Minimum-redundancy linear arrays," *IEEE Transactions on Antennas and Propagation*, vol. 16, no. 2, pp. 172–175, 1968.

[6] Palghat P. Vaidyanathan and Piya Pal, "Sparse sensing with co-prime samplers and arrays," *IEEE Transactions on Signal Processing*, vol. 59, no. 2, pp. 573–586, 2011.

[7] Saeid Sedighi, Bhavani Shankar Mysore Rama Rao, and Björn Ottersten, "An asymptotically efficient weighted least squares estimator for co-array-based doa estimation," *IEEE Transactions on Signal Processing*, vol. 68, pp. 589–604, 2020.

[8] Umesh Sharma and Monika Agrawal, "Third-order nested array: An optimal geometry for third-order cumulants based array processing," *IEEE Transactions on Signal Processing*, vol. 71, pp. 2849–2862, 2023.

[9] Ryan Haoyun Wu, "Distributed Aperture Automotive Radar System with Alternating Master Radar Devices," European Patent EP 3 712 653 A1, Sep. 2020.

[10] Stephen Crouch and Chunshu Li, "Virtual Antenna Array with Distributed Aperture," U.S. Patent 11,899,127 B2, Feb. 2024.

[11] Ryan Haoyun Wu, Filip Alexandru Rosu, Daniel Silion, and Tudor Bogatu, "Automotive MIMO Radar System Using Efficient Difference Co-Array Processor," U.S. Patent 11,888,554 B2, Jan. 2024.

[12] Moein Ahmadi, Mohammad Alaee-Kerahroodi, Linlong Wu, Bhavani Shankar M. R., and Björn Ottersten, "Detector Design for Distributed Multichannel Radar Sensors in Colored Interference Environments," in *ICASSP 2024*, 2024, pp. 8531–8535.

[13] P. Stoica, Zhisong Wang, and Jian Li, "Robust capon beamforming," *IEEE Signal Processing Letters*, vol. 10, no. 6, pp. 172–175, 2003.

[14] D. Malioutov, M. Cetin, and A.S. Willsky, "A sparse signal reconstruction perspective for source localization with sensor arrays," *IEEE Transactions on Signal Processing*, vol. 53, no. 8, pp. 3010–3022, 2005.